

Developmental Testbed Center (DTC) Visitor Program 2017

**Evaluation of the Newly Developed Observation Operators for
Assimilating Satellite Cloud Precipitation Observations in GSI
within HWRF system**

Ting-Chi Wu

Cooperative Institute for Research in the Atmosphere
Colorado State University
Fort Collins, CO 80523
E-mail: ting-chi.wu@colostate.edu

Final Project Report
31 July 2018

1. Introduction

Clouds and precipitation are part of the dynamics of hurricane processes. Increased cloud and precipitation observations available from the microwave sensors aboard the Global Precipitation Measurement mission (GPM) satellite may be utilized to improve hurricane forecast skills. Among these observations, all-sky satellite radiances and retrieved hydrometeors are especially important because they contain information about clouds and precipitation that often occur in sensitive regions in terms of forecast impact. However, NOAA's operational Hurricane Weather Research and Forecasting (HWRF) system currently excludes observations indicative of clouds and precipitation from their assimilation routine. As a preliminary attempt toward assimilating cloud and precipitation information in HWRF, satellite retrieved hydrometeor observations from GPM are introduced to HWRF in the study herein.

The goal of the project is to increase the utility of satellite measurement of cloud and precipitation information into HWRF by adding the capability in the data assimilation component of HWRF, which utilizes the Gridpoint Statistical Interpolation (GSI), to assimilate satellite retrieved hydrometeor data into the HWRF system. The added capability includes the implementation of two pairs of observation operators and their corresponding tangent linear and adjoint parts. Two Atlantic hurricane cases – Edouard and Gonzalo (both occurred in 2014) – are selected to perform two HWRF-GSI experiments to examine the impact of added capability on the analysis and the subsequent forecast of HWRF.

2. Data

2.1 Hydrometeor Retrievals – Hurricane GPROF

Building from the Goddard PROFiling algorithm (GPROF, Kummerow et al. 2015), a customized retrieval algorithm for hurricane application was developed and referred to as Hurricane GPROF (Brown et al. 2016). Hurricane GPROF algorithm improves the latest GPROF (version 2014) retrievals in hurricane scenes by utilizing a combination of 1) an a priori database that contains rain rates measured by precipitation radar (PR) onboard the Tropical Rainfall Measuring Mission (TRMM) and the brightness temperatures measured by TRMM Microwave Imager (TMI), 2) best-track information that contains storm location and horizontal extent of 34-kt wind from the HURricane DATA 2nd generation (HURDAT2) dataset, and 3) the GPROF 2014 retrieval algorithm. Finally, the Hurricane GPROF retrieval algorithm provides retrieved instantaneous rain rates and vertical profiles of four hydrometeor types for tropical storm pixels. Since the architecture of TMI and the GPM Microwave Imager (GMI) was similar enough, Hurricane GPROF algorithm was also applied to GMI for rain rate and hydrometeor profile retrievals.

2.2 Preparation for Assimilation

To ease the assimilation efforts, the four hydrometeor profiles, which include cloud water, rain, mixed-phase, and ice, are transformed into two vertically integrated quantities: solid-water content path (SWCP) and liquid-water content path (LWCP). SWCP is formed by first adding values of the upper-half of the mixed-phase profile to the corresponding values of the ice profile. The added profile is then vertically integrated. For LWCP, the integral is also an added profile, which is formed by adding values

of the lower-half of the mixed-phase profile to the corresponding values of the rain and cloud water profiles. An example of the SWCP and LWCP valid at 1200 UTC 16 October during Hurricane Gonzalo (2014) is shown in Fig. 1.

The SWCP and LWCP retrievals described here are sensitive to developed convective systems, and are available over ocean only. As such, they can be viewed as complementary to all-sky satellite radiances, which are found to be more effective in depicting the early stage of a storm, as well as to radar-based water content retrievals, which are available only near land.

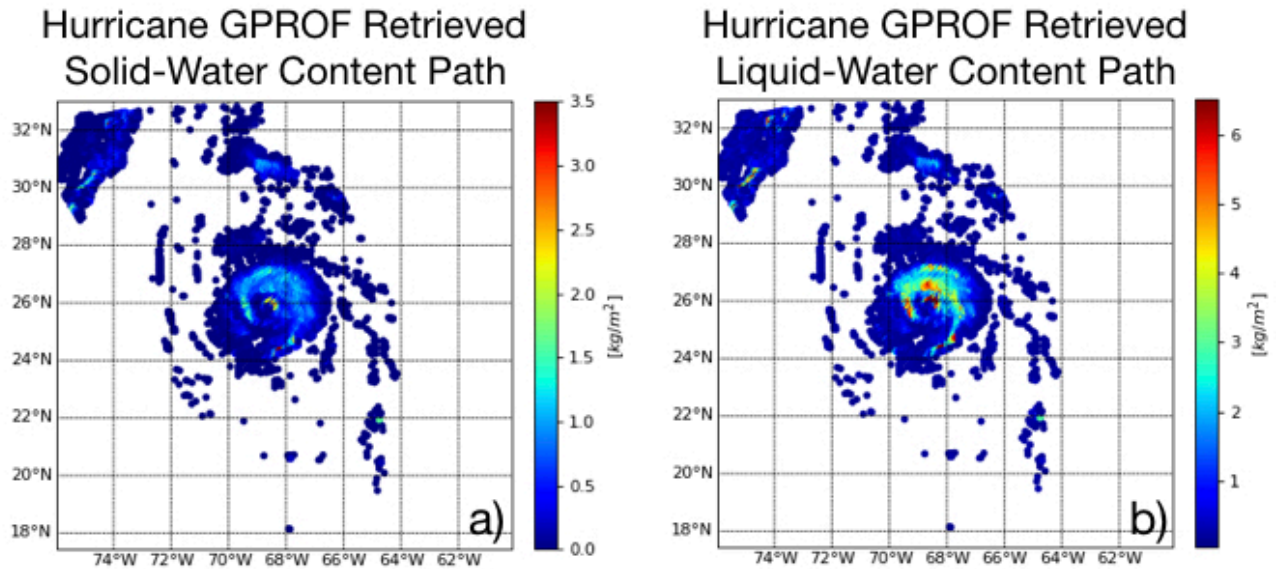


Figure 1. Hurricane GPROF retrieved a) SWCP (kg m^{-2}) and b) LWCP (kg m^{-2}) valid at 1200 UTC 16 October during Hurricane Gonzalo (2014). Retrieved data are plotted on the innermost domain of HWRP, which is centered on the position of the hurricane.

3. Methodology

3.1 HWRP System

The community release version 3.9a of HWRP, which is functionally equivalent to the 2017 operational HWRP, is employed in this study. Figure 2 is a simplified overview of the HWRP system, which is composed of three major components. They are 1) an initialization component that includes a pre-processing step to initialize all five domains (three forecast domains and two data assimilation domains that are referred to as ghost domains 2 and 3) with the use of GFS and GDAS data, a vortex improvement (also known as vortex initialization) procedure that corrects the intensity, location, and size of either a tropical storm vortex from a previous HWRP forecast or a bogus vortex based on the Tropical Cyclone Vitals Database (TCVitals), and a data assimilation system that utilizes the GSI, 2) a forecasting component that is composed of the Nonhydrostatic Mesoscale Model (NMM) dynamical core of WRF and the Princeton Ocean Model of Tropical Cyclone (POM-TC) model combined by the NCEP coupler, and 3) a post-processing package that includes the Unified Post-Processing (UPP) and Geophysics Fluid Dynamic Laboratory (GFDL) vortex tracker.

Among the various HWRF physics packages, cloud microphysics scheme is most directly related to the assimilation of hydrometeor retrievals because microphysics parameterization explicitly handles the behavior of cloud hydrometeors. The Ferrier-Aligo microphysics scheme (Aligo et al. 2014) is employed by HWRF. It predicts changes in water vapor and hydrometeor species that include cloud liquid water, rain, cloud ice, and the precipitating ice (snow, graupel, and sleet), but only considers the advection of water vapor and the combined sum of hydrometeor species, which is referred to as total cloud condensate (CWM). As a result, CWM is the prognostic variable instead of individual hydrometeor species. Using CWM and three partition parameters that include fraction of rain (F_RAIN), fraction of ice (F_ICE), and riming rate (F_RIMEF), individual hydrometeor species can then be diagnosed at output time.

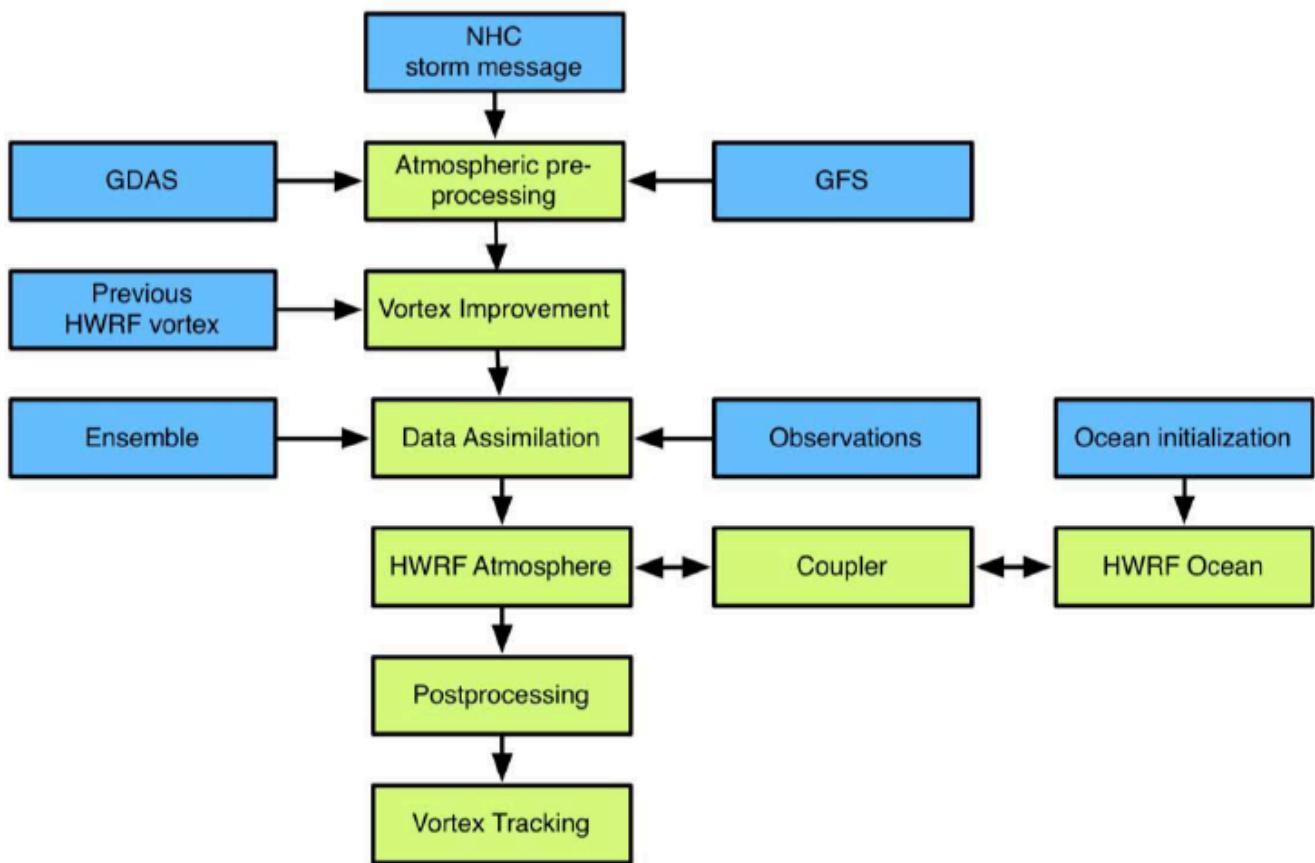


Figure 2. A simplified flowchart of the HWRF system.

This project will focus on the data assimilation component of HWRF. New capabilities are implemented in GSI to enable the assimilation of SWCP and LWCP in HWRF.

3.2 Observation Operators for SWCP and LWCP

In order to assimilate SWCP and LWCP into HWRF with GSI, new observation operator is needed. Wu et al. (2016) developed a pair of observation operators to assimilate SWCP and LWCP based on the

assumption that water vapor in excess of saturation will condense out. That is, the operator for SWCP is a vertical integral of super-saturated water vapor with respect to ice, referred to as h_s and expressed as

$$h_s = \sum_{k=k_0}^{k_{\max}} \left[\left(\frac{q^k}{1-q^k} \right) - 0.622 \frac{e_s(T^k)}{P^k - e_s(T^k)} \right] \cdot \frac{\Delta P^k}{g} \quad (1)$$

and the operator for LWCP is a vertical integral of super-saturated water vapor with respect to liquid, referred to as h_l and expressed as

$$h_l = \sum_{k=1}^{k_{\text{mix}}} \left[\left(\frac{q^k}{1-q^k} \right) - 0.622 \frac{e_s(T^k)}{P^k - e_s(T^k)} \right] \cdot \frac{\Delta P^k}{g} \quad (2)$$

where T is temperature, P is pressure, q is specific humidity, e_s is saturation vapor pressure, the superscript k denotes the model level index, k_0 is the vertical level where temperature is $T_0=273.15\text{K}$, k_{mix} is the vertical level where temperature is $T_{\text{mix}}=253.15\text{K}$, k_{max} is the index for the top model level, ΔP_k is pressure difference between two vertical levels k and $k+1$, and g is the acceleration due to gravity.

This pair of observation operators (Eqs. 1-2) is implemented in GSI for the assimilation of SWCP and LWCP with the intention to adjust the environment to support the existence of cloud condensate without introducing new cloud control variable. Following Eqs. 1-2, environmental temperature will decrease and specific humidity will increase to reach a super-saturated state as if there is an increase in cloud condensate. In addition to the observation operators, their tangent linear and adjoint parts are also implemented, as they are expected by the cost function minimization iteration. More details regarding the tangent linear and adjoint equations can be found in the appendix in Wu et al. (2016).

In order to align with the GSI all-sky radiance assimilation efforts, a new development to directly utilize cloud condensate within data assimilation is motivated. Wu and Zupanski (2017) modified the HWRP system to allow cloud condensate cycling and developed a new pair of observation operators that use the HWRP microphysical cloud condensate variables for the assimilation of hydrometeor retrievals. In the new pair of observation operators, SWCP is a vertical integral of solid hydrometeor species that include cloud ice, snow, graupel, and hail (if all exist). Such operator is referred to as h_s_Hydro and can be expressed as

$$h_{s_Hydro} = \sum_{k=k_0}^{k_{\max}} (q_i^k + q_s^k + q_g^k + q_h^k) \cdot \frac{\Delta P^k}{g} \quad (3)$$

Similarly, the operator for LWCP is a vertical integration of the liquid hydrometeor species that include cloud liquid water and rain, and is referred to as h_l_Hydro with the following expression

$$h_{l_Hydro} = \sum_{k=1}^{k_{\text{mix}}} (q_l^k + q_r^k) \cdot \frac{\Delta P^k}{g} \quad (4)$$

where q_l , q_i , q_r , q_s , q_g , and q_h are mixing ratio of cloud liquid water, cloud ice, rain water, snow, graupel, and hail, respectively.

3.3 Modifications to HWRF for Cloud Condensate Cycling

In order to use cloud condensate variables in the h_s_Hydro and h_l_Hydro observation operators, three major modifications to HWRF are required and they are 1) establishing a first guess field with non-zero cloud condensate, 2) adding CWM as a control variable and individual cloud hydrometeors as state variables to allow cloud condensate update during data assimilation, and 3) incorporate a partition algorithm to decompose CWM into individual hydrometeor species along with the tangent linear and adjoint parts of the partition in GSI.

The first modification is required because the current vortex initialization procedure excludes cloud condensate variables during the intensity, location, and size adjustment routine. As a result, the outcome of vortex initialization is a first guess with constant values of zero in the CWM, F_ICE, F_RAIN, and F_RIMEF fields. In order to avoid a cloud-absent (i.e., clear sky) first guess, a quick fix was proposed to replace pre-existing zeros by establishing values of CWM and the three partition parameters using the values from the same fields in the 6-h forecast of a previous HWRF cycle. During the quick fix, center relocation is considered to avoid a spatial shift between the re-established cloud condensate fields and other fields that already exist in the first guess.

The second modification is also required because the current HWRF does not consider cloud condensate variable update during the GSI data assimilation. Adding CWM as a control variable and the six cloud hydrometeor species as state variables will allow the h_s_Hydro and h_l_Hydro observation operators to function and at the same time enable the update of cloud condensate variables.

Finally, a partition algorithm that decomposes CWM into individual cloud hydrometeors is included as part of implementation of the h_s_Hydro and h_l_Hydro observation operators. Such partition algorithm is an empirical formulation based on the Ferrier-Aligo microphysics scheme. Description of the partition is provided in below. The very first step of the partition algorithm is to use F_ICE to determine the solid and liquid phases of CWM:

$$\text{the solid phase of CWM} = F_ICE \cdot CWM \quad (5)$$

and

$$\text{the liquid phase of CWM} = (1 - F_ICE) \cdot CWM \quad (6)$$

Then, F_RAIN is used to further partition the liquid phase of CWM into q_l and q_r as

$$q_l = (1 - F_RAIN) \cdot (1 - F_ICE) \cdot CWM \quad (7)$$

and

$$q_r = F_RAIN \cdot (1 - F_ICE) \cdot CWM \quad (8)$$

On the other hand, the solid phase of CWM is decomposed into q_i and $precip_ice$ as

$$q_i = w \cdot F_ICE \cdot CWM \quad (9)$$

and

$$precip_ice = (1 - w) \cdot F_ICE \cdot CWM \quad (10)$$

where $precip_ice$ is precipitating ice as opposed to q_i being the non-precipitating ice, using an empirical weighting coefficient w

$$w = \begin{cases} 0.05 \cdot \frac{T - T_2}{T_1 - T_2} + 0.1 \cdot \frac{T - T_1}{T_2 - T_1} & \text{if } T \leq T_1 \\ 0.05 & \text{if } T > T_1 \end{cases} \quad (11)$$

where T is temperature, $T_1 = 243.15\text{K}$, and $T_2 = 233.15\text{K}$. Finally, depending on the value of F_RIMEF , $precip_ice$ is equal to q_s , q_g , or q_h :

$$precip_ice = \begin{cases} q_s & \text{if } 1 \leq F_RIMEF \leq 5 \\ q_g & \text{if } 5 < F_RIMEF \leq 20 \\ q_h & \text{if } F_RIMEF > 20 \end{cases} \quad (12)$$

As mentioned earlier, the tangent linear and adjoint parts of this partition algorithm are also included in GSI within the cost function minimization procedure.

In summary, the three modifications together facilitate the cloud condensate cycling in HWRF by first preparing a guess field with realistic cloud condensate values and then updating the cloud condensate values via data assimilation of cloud-related observations.

4. Experimental Design

The 2017 HWRF operational configuration (Biswas et al. 2017) is adapted in this study. In short, the data assimilation portion of the 2017 HWRF operational configuration includes the use of a hybrid ensemble-variational GSI-based data assimilation scheme on the two ghost domains. For both ghost domains, 20% of the weight is given to static covariance, while 80% of the weight is given to the HWRF ensemble covariance. The horizontal localization scale is set to 300 km and 150 km for ghost domain 2 and ghost domain 3 respectively. There are total of two outer loops and each outer loop has 50 inner iterations. The control variables include stream function, unbalanced part of velocity potential, unbalanced part of temperature, unbalanced part of surface pressure, normalized relative humidity, and surface skin temperature. Conventional observations contained in PrepBUFR file are assimilated in both ghost domains 2 and 3. In addition, NOAA P3 aircraft Tail Doppler Radar, high resolution flight-level data, Atmospheric Motion Vectors from GOES, satellite radiances from CrITS, SSMIS, Metop-B, AMSU-A, Metop-B MHS, and IASI are also assimilated in both ghost domains. Finally, HS3 Global Hawk dropsonde and TCVital mean sea-level pressure data are included as well.

Two data assimilation experiments are conducted to examine the performance of assimilating the retrieved SWCP and LWCP from the Hurricane GPROF algorithm in the ghost domain 3 of HWRf. The corresponding descriptions for the two experiments are:

- (i) The NOHYDRO experiment, which follows the 2017 HWRf operational configuration and assimilates SWCP and LWCP retrievals in the ghost domain 3 of HWRf using h_s and h_l .
- (ii) The HYDRO experiment, which utilizes a modified HWRf (see section 3.3) to allow cloud condensate cycling and assimilates SWCP and LWCP retrievals in the ghost domain 3 of HWRf using h_{s_Hydro} and h_{l_Hydro} .

Two hurricanes were selected to perform the two above-mentioned experiments, and they are Hurricane Edouard (AL06) and Hurricane Gonzalo (AL08). There are a total of 4 runs (2 experiments x 2 cases) and they are summarized in Table 1.

Hurricane Case	Experiments	Experiment Period
Edouard (AL06)	HYDRO and NOHYDRO	2014/09/16 0000 UTC – 2014/09/17 0600 UTC
Gonzalo (AL08)	HYDRO and NOHYDRO	2014/10/16 0600 UTC – 2014/10/17 0600 UTC

Table 1. All 4 HWRf runs from the two hurricane cases

For the Edouard case, the Hurricane GPROF retrievals were available at 0600 UTC 16 September and 0600 UTC 17 September. Due to the data availability, the experiment period starts 6 hour before the first data was valid and ends at the time when the last data was valid. As for the Gonzalo case, the retrievals were available at 1200 UTC 16 October and 0600 UTC 17 October. Therefore, the experiment period starts at 0600 UTC 16 October and ends at 0600 UTC 17 October.

5. Results

5.1 Observed vs. Simulated (Background and Analysis)

In the NOHYDRO experiment, the background guess values of both SWCP and LWCP (Figs. 3a and 4a) appear to be lower than observations (Fig. 1). Although the corresponding analysis fields are an improvement over their background guess, there exists a negative bias due to the use the h_s and h_l operators.

It was pointed out in Wu et al. (2016) that a potential negative bias is expected because the first guess fields have already gone through saturation followed by condensation. During the HWRf integration, microphysics and/or cumulus parameterization has already condensed out a portion of super-saturated water vapor. As a consequence, water vapor in excess of saturation computed from the h_s and h_l operators using the saturated-then-condensed first guess fields is much reduced. Due to this potential

negative bias and the lack of cloud condensate update, the development of h_{s_Hydro} and h_{l_Hydro} operators was motivated.

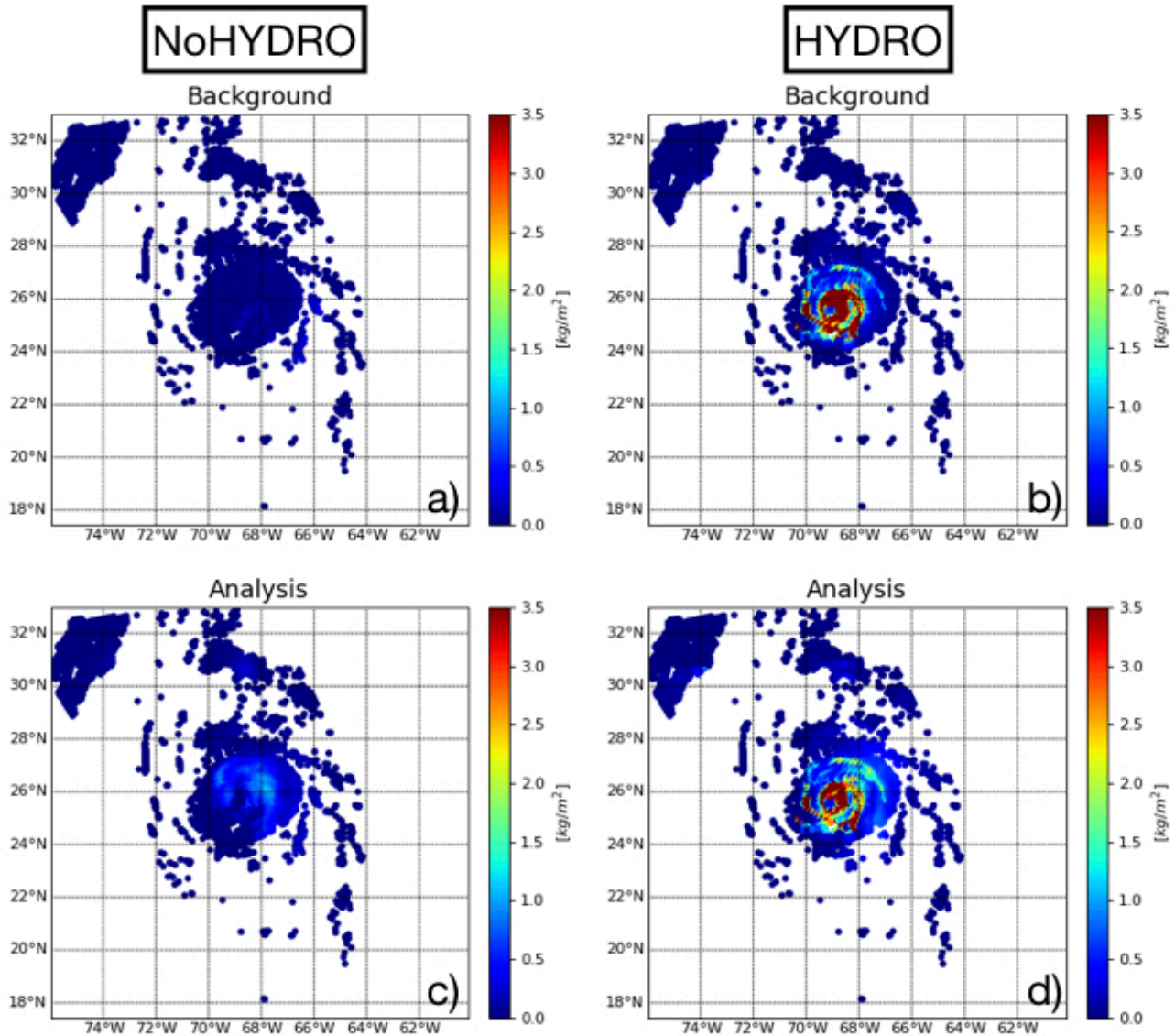


Figure 3. Similar to Fig. 1a, but for the HWRf-GSI background guess of SWCP (kg m^{-2}) from a) the NOHYDRO experiment and b) the HYDRO experiment, and the HWRf-GSI analysis of SWCP (kg m^{-2}) from c) the NOHYDRO experiment and d) the HYDRO experiment.

Unlike results from the NOHYDRO experiment, background guess values of SWCP and LWCP in the HYDRO experiment are a result of vertical integration of cloud condensate. Using the h_{s_Hydro} and h_{l_Hydro} operators with cloud condensate cycling appears to produce, in general, background guess values of SWCP (Fig. 3b) that are much higher than observations within the core of Hurricane Gonzalo. In contrast, background guess values of LWCP in the HYDRO experiment (Fig. 4b) are lower than observations. Although the analysis fields of both SWCP and LWCP (Figs. 3d and 4d) are a better fit to observations compared to their corresponding background fields, the adjustments are different: one acts

toward reducing solid water condensate while the other indicates an increase of liquid water condensate. Since CWM (total cloud condensate) is the control variable instead of each individual hydrometeor species, the response is expected to be realized through a reduction of CWM in the upper levels and an increment of CWM in the lower levels.

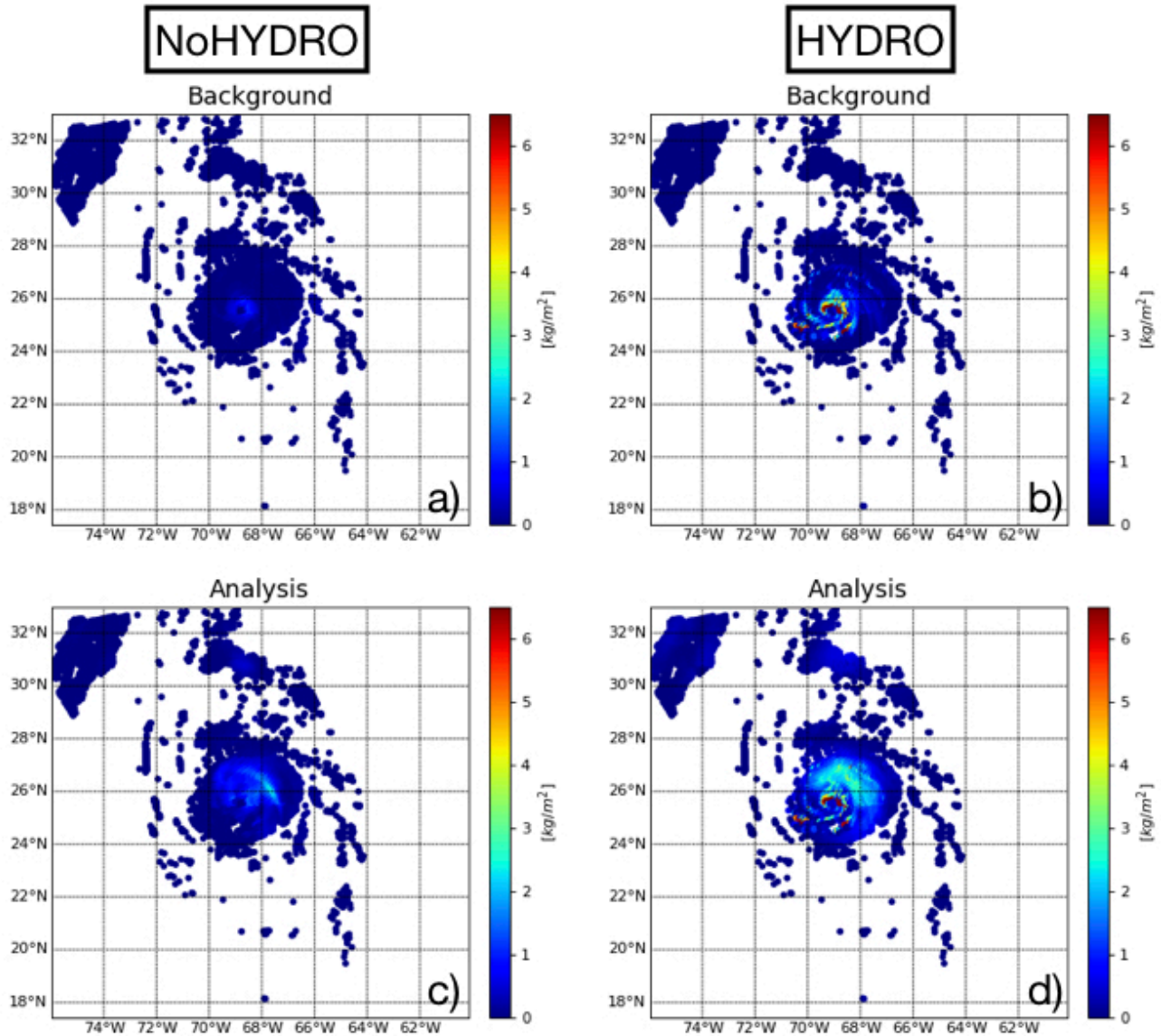


Figure 4. Similar to Fig.3, but for LWCP ($kg\ m_{.2}$).

5.2 Analysis Increment

The aforementioned adjustments from background to analysis can be further understood through analysis increment (analysis minus background) in model space. A vertical cross section of analysis increments in total cloud condensate, specific humidity, and temperature from both NOHYDRO and HYDRO experiments along a east-west cross section at 26 °N is displayed. As was expected, there is zero increment in CWM in the NOHYDRO experiment (Fig. 5a). In the HYDRO experiment, there

appears to be a general reduction of CWM in the upper levels (> 500 mb) and an increase of CWM in the lower levels along the vertical columns between 70°W and 67.5°W in Fig. 5d. This is consistent with our findings in Figs. 3 and 4.

In general, the pattern of the increments in specific humidity and temperature is similar between the two experiments, except that the magnitude is slightly larger in the HYDRO experiment. For example, the maximum increment in specific humidity is $\sim 2 \text{ g kg}^{-1}$ in the NOHYDRO experiment, while the corresponding maximum is $\sim 4.5 \text{ g kg}^{-1}$ in the HYDRO experiment. This larger response in terms of magnitude is the result of larger innovation (differences between background guess and observation).

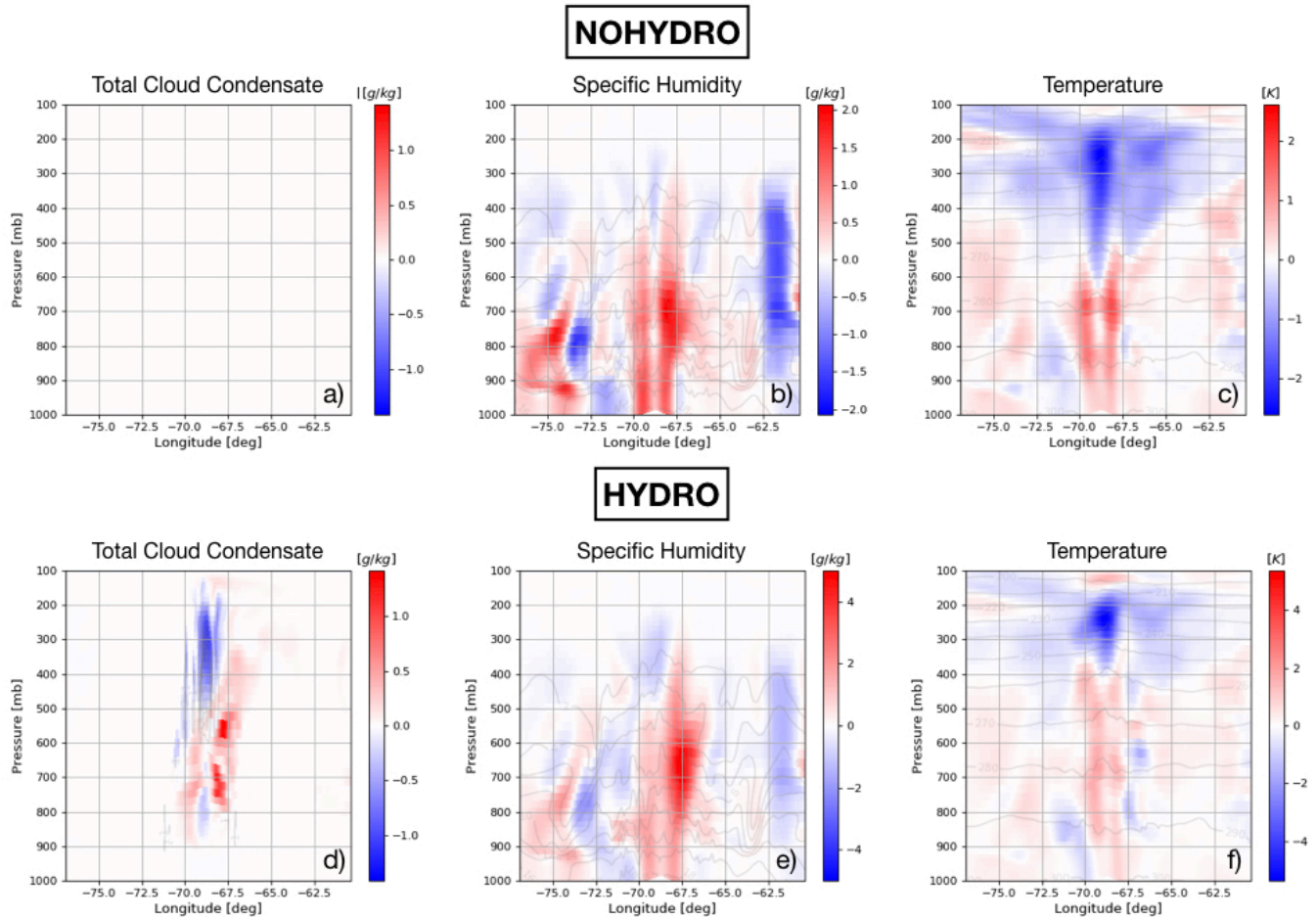


Figure 5. An east-west vertical cross-section of analysis increments in a) total cloud condensate (CWM; g/kg), b) specific humidity (g/kg), and c) temperature (K) from the NOHYDRO experiment valid at 12 UTC 16 October for Hurricane Gonzalo. d)-f) are the same as a)-c), except for increments from the HYDRO experiment. In each sub figure, the corresponding background field is plotted in gray contour. The vertical cross-section is along 26°N .

5.3 Evaluate with Microwave Brightness Temperatures

Observed imagery from the GPM Microwave Imager (GMI) is used to further evaluate an analysis field. As part of the GSI forward operator, the Community Radiative Transfer Model (CRTM) is used to

compute brightness temperatures from a given atmospheric state. To begin with, the background and analysis fields from the HYDRO experiment are passed to the CRTM to generate synthetic GMI imagery.

A side-by-side comparison of observed GMI imagery at 36.5 GHz and the synthetic imagery from the background and the analysis fields are displayed in Figs. 6a-c respectively. In Fig. 6a, the observed microwave imagery at 36.5 GHz is generally cold (brightness temperature < 240 K) over the oceans with clear sky, while the imagery appears warm (brightness temperature > 260 K) when cloud signatures are present. In general, the synthetic imagery of background has a cloud feature (Fig. 6b) that is slightly smaller than the observed, while the synthetic imagery of analysis is supported by observations. Similar to Figs. 6a-c, a side-by-side comparison of observed GMI imagery at 89 GHz and the synthetic imagery from the background and the analysis fields are displayed in Figs. 6d-f. Unlike microwave imagery at 36.5 GHz, the observed microwave imagery at 89 GHz is generally warm (brightness temperature > 270 K) over the oceans with clear sky, while the imagery appears cold (brightness temperature < 250 K) when cloud signatures are present. Synthetic imagery of the background appears to have cloud signatures that cover a much smaller horizontal region than the observed imagery (Fig. 6d-e). Although the synthetic imagery of analysis has shown a horizontal cloud coverage that is similar to the observed one, there are not enough cold cloud pixels (brightness temperature < 230 K).

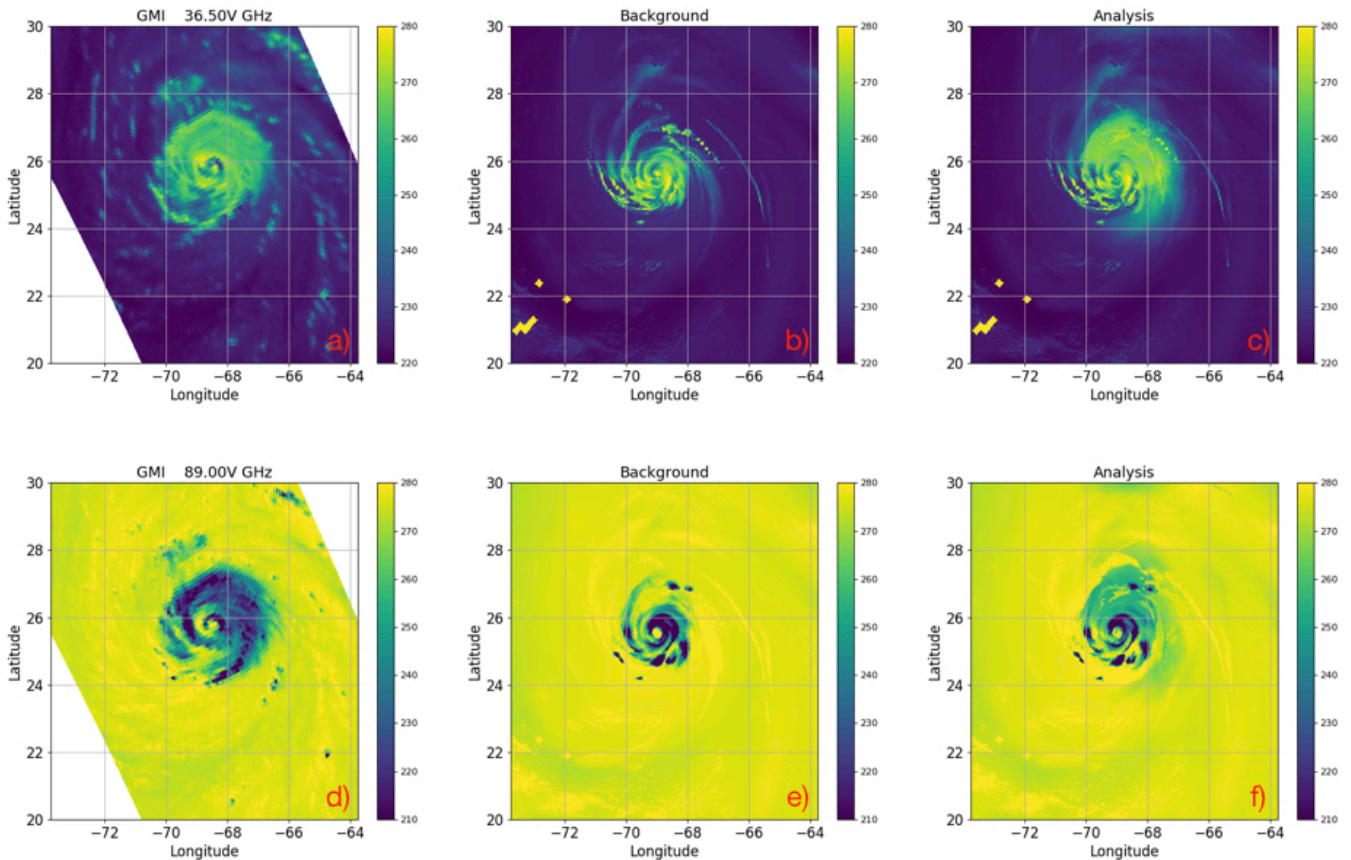


Figure 6. a) GMI 36.5 GHz microwave imagery and synthetic satellite images (brightness temperature in K) of b) background and c) analysis from the HYDRO experiment valid at 1200 UTC 16 October. d)-f) are the same as a)-c), except for GMI 89 GHz microwave imagery.

5.4 Impact on HWRP Forecast

For completeness of the study, an HWRP forecast is carried out for both experiments. A 72-h HWRP forecast initialized from 0600 UTC 17 October for both HYDRO and NOHYDRO runs for the Gonzalo case is conducted. This is because Gonzalo lost its tropical feature and dissipated into an extra-tropical system after 19 October. As a consequence, there is no best track data available beyond 72 hours from the initialization time. Similarly, a 120-h HWRP forecast initialized from 0600 UTC 17 September for both HYDRO and NOHYDRO runs for the Edouard case is carried out as well. In Fig. 7, a summary of the track forecast, track error, and intensity forecast in terms of minimum sea level pressure is presented. However, a statistical inference about the impact of assimilating Hurricane GPROF hydrometeor retrievals on the subsequent forecast could not be made until more cases are used (sample size too small).

A recent study by Wu et al. (2018) assimilates all-sky microwave radiances into HWRP with cloud condensate cycling. The cloud signatures in the analysis of the case study (Hurricane Cristobal 2014) were supported by observations. However, they found that due to the absence of upward vertical motion, during the first 30 minutes of the forecast, cloud condensate field experiences evaporation and precipitation settling (see Fig. 14 in Wu et al. 2018). Similarly, this study assimilates Hurricane GPROF hydrometeor retrievals and produces an analysis field with cloud condensate features that are supported by observations (Fig. 6). Both studies point out that further development on the HWRP architecture is required in order to allow realistic vertical motions to support the cloud condensate field in the initial time.

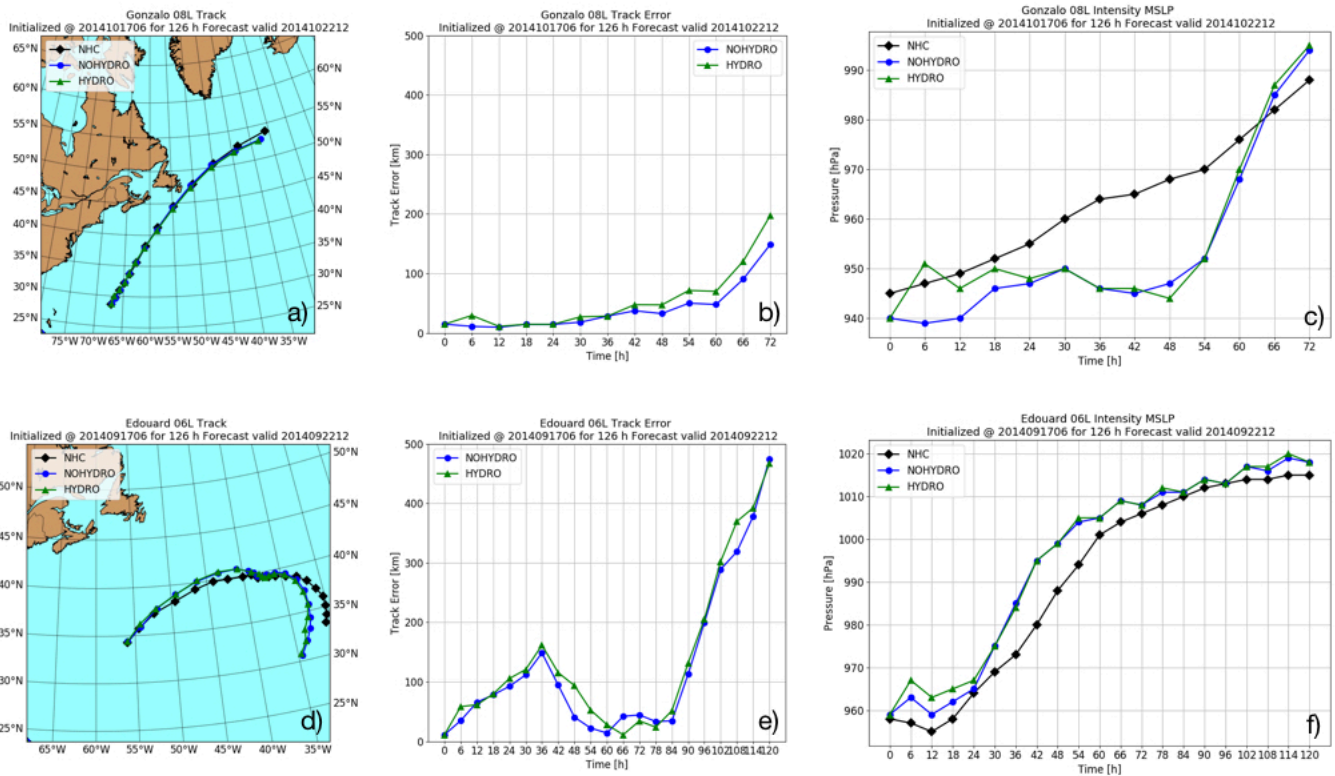


Figure 6. a) HWRF forecast track, b) track error (km), and c) minimum central sea-level pressure (hPa) from the HYDRO and NOHYDRO experiments for the Gonzalo case initialized at 0600 UTC 17 October. d)-f) are the same as a)-c), except for the Edouard case initialized at 0600 UTC 17 September.

6. Deliverables

6.1 Merge to EMC GSI Trunk

The capability to assimilate Hurricane GPROF retrieved SWCP and LWCP, which include both pairs of observation operators and their corresponding tangent linear and adjoint parts, has been implemented and committed to the top of the GSI trunk as of January 2018. Since then, the added capability has passed the regression test and gained approval by the DA Review Committee. As of the writing, the added capability is now available to be used by the community.

Here is a list of the newly added codes:

Name of Fortran Code	Description
read_wcpbuf.f90	read both swcp and lwcp from one wcpbuf file
m_swcpNode.f90 & m_lwcpNode.f90	extend obsNode to include swcp and lwcp
setupswcp.f90 & setuplwcp.f90	full nonlinear operators and diagnostics are saved in conv
intswcp.f90 & intlwcp.f90	linear and adjoint operators
stpswcp.f90 & stplwcp.f90	step length calculation

A logical variable *l_wcp_buf* inside the &SETUP section of the *gsiparm.nml* namelist is used to determine which pairs of observation operators (HYDRO or NOHYDRO) and their corresponding linear/adjoint operators along with their step length calculations will be used. If *l_wcp_buf* is set to .true., then HYDRO will be used, otherwise, NOHYDRO will be used.

Here is a list of the existing codes that were modified due to the new implement:

Name of Fortran Code	Modifications
gsimod.F90	add <i>l_wcp_cwm</i> as a new logical variable in <i>gsiparm.nml</i> namelist
intjo.f90	add call to <i>intswcp</i> and <i>intlwcp</i>
m_obsdiags.F90	add use <i>m_swcpNode</i> and <i>m_lwcpNode</i> add <i>swcphead</i> and <i>lwcphead</i> pointers
m_obsHeadBundle.F90	add use <i>m_swcpNode</i> and <i>m_lwcpNode</i> add <i>swcp</i> and <i>lwcp</i> pointer add use <i>swcphead</i> and <i>lwcphead</i> pointer add <i>yobs%swcp</i> and <i>yobs%lwcp</i>
obsmod.F90	add <i>swcphead/swcptail</i> and <i>lwcphead/lwcp</i> add <i>iout_swcp</i> and <i>iout_lwcp</i> add <i>mype_swcp</i> and <i>mype_lwcp</i> add <i>i_swcp_ob_type</i> and <i>i_lwcp_ob_type</i>
read_obs.F90	add call to <i>read_wcpbuf</i> if <i>obstype</i> is either <i>swcp</i> or <i>lwcp</i>

setuprhsall.f90	add call to setupswcp and setuplwcp
statsconv.f90	add summary report for swcp and lwcp in conv
stpjo.f90	add call to stpswcp and stplwcp add yobs%swcp and yobs%lwcp association
Makefiles	
Makefile	Add dependency due to newly added code
Makefile.dependency	
Makefile.src	

Finally, here is a list of existing codes that were modified specifically for the HYDRO operators due to the use of total cloud condensate (CWM):

Name of Fortran Code	Modifications
cwhydromod.f90	add subroutines <i>cw2hydro_tl_hwrf</i> and <i>cw2hydro_ad_hwrf</i> as they contain the tangent linear and adjoint parts of the CWM partition (Eqs. 5-12)
control2state.f90	add call to <i>cwhydro_tl_hwrf</i> and increase nsvars from 8 to 12 add <i>qr</i> , <i>qs</i> , <i>qg</i> , and <i>qh</i> to mysvars (<i>ql</i> and <i>qi</i> were already listed)
control2state_ad.f90	add call to <i>cwhydro_ad_hwrf</i> and increase nsvars from 8 to 12 add <i>qr</i> , <i>qs</i> , <i>qg</i> , and <i>qh</i> to mysvars (<i>ql</i> and <i>qi</i> were already listed)
ensctl2state.f90	the same modifications that were made to control2state.f90
ensctl2state_ad.f90	the same modifications that were made to control2state_ad.f90
cplr_read_wrf_nmm_guess.f90	add <i>gsi_bundlegetpointer</i> call to load <i>ges_fice</i> , <i>ges_frain</i> , and <i>ges_frimef</i> in subroutine <i>read_wrf_nmm_netcdf_guess_wrf</i> so that they can be later used by cwhydromod.f90
cplr_wrwrfnmma.f90	in subroutine <i>wrwrfnmma_netcdf_wrf</i> , add 1) read in guess field of <i>CWM</i> , <i>F_ICE</i> , <i>F_RAIN</i> , and <i>F_RIMEF</i> , 2) update guess field of <i>CWM</i> , <i>F_ICE</i> , <i>F_RAIN</i> , and <i>F_RIMEF</i> with analysis increments, and 3) write out updates fields of <i>CWM</i> , <i>F_ICE</i> , <i>F_RAIN</i> , and <i>F_RIMEF</i>
get_gefs_for_regional.f90	allow ensemble perturbations of CWM to be loaded
compute_qvar3d.f90	add <i>gsi_bundlegetpointer</i> to acquire <i>ges_qr</i> , <i>ges_qs</i> , <i>ges_qg</i> , and <i>ges_qh</i> so that the updated <i>CWM</i> is a summation of all four of them plus <i>ges_qi</i> and <i>ges_ql</i>
update_guess.f90	the same modifications that were made to compute_qvar3d.f90

6.2 Instructions to use the Capability

In order to assimilate Hurricane GPROF retrieved SWCP and LWCP using either pairs of observation operators (HYDRO or NOHYDRO) in GSI, one needs to prepare a bufr file that contains both the SWCP and LWCP data (instruction can be provided upon request). If such a bufr file exists, it has to be renamed to *wcpbufr* in order to be recognized by GSI. Finally, below is a list of required modifications to three GSI input/fix file in order to activate the capability:

1. *convinfo*: include swcp and lwcp as part of conventional observations

```

swcp 162 0 1 3.0 0 0 0 10.0 8.0 2.0 10.0 0.000000 0 0. 0. 0 0. 0.
lwcp 162 0 1 3.0 0 0 0 10.0 8.0 2.0 10.0 0.000000 0 0. 0. 0 0. 0.

```

2. *gsiparm.nml*: include *swcp* and *lwcp* in the &OBS_INPUT list

```

wcpbufr swcp null swcp 0.0 0 0
wcpbufr lwcp null lwcp 0.0 0 0

```

and include the *l_wcp_bufr* option in the &SETUP section (default is .false.)

```

l_wcp_bufr = .true. ! operator HYDRO
l_wcp_bufr = .false. ! operator NOHYDRO

```

3. *anavinfo*: when *l_wcp_bufr* = .true., include *cw* and its partition parameters (*fice*, *frain*, and *frimef*), and the six distinct hydrometeor habits (*q_b*, *q_i*, *q_s*, *q_r*, *q_g*, and *q_h*) in *met_guess* bundle

```

met_guess::
!var level crtm_use desc orig_name
ps 1 -1 surface_pressure ps
z 1 -1 geopotential_height phis
u 60 2 zonal_wind u
v 60 2 meridional_wind v
tv 60 2 virtual_temperature tv
q 60 2 specific_humidity sphu
oz 60 2 ozone ozone
pint 61 -1 nmm_pressure pint
pd 1 -1 nmm_del_pressure pd
cw 60 10 cloud_condensate cw
fice 60 -1 ice_fraction fice
frain 60 -1 rain_fraction frain
frimef 60 -1 riming_rate frimef
ql 60 12 cloud_condensate ql
qi 60 12 cloud_condensate qi
qr 60 12 cloud_condensate qr
qs 60 12 cloud_condensate qs
qg 60 12 cloud_condensate qg
qh 60 12 cloud_condensate qh
::

```

and include *cw* as control variable and the six distinct hydrometeor habits as state variables

```

control_vector::
!var level itracer as/tsfc_sdv an_amp0 source func0f
sf 60 0 0.2 -1.0 state u,v
vp 60 0 0.2 -1.0 state u,v
ps 1 0 0.30 -1.0 state prse
t 60 0 0.70 -1.0 state tv
q 60 1 0.20 -1.0 state q
cw 60 1 1.00 -1.0 state cw
oz 60 1 0.10 -1.0 state oz
sst 1 0 1.00 -1.0 state sst
stl 1 0 1.00 -1.0 motley sst
sti 1 0 1.00 -1.0 motley sst
::

```

```

state_vector::
!var      level  itracer source      funcf
u         60     0     met_guess  u
v         60     0     met_guess  v
tv        60     0     met_guess  tv
tsen      60     0     met_guess  tv,q
q         60     1     met_guess  q
oz        60     1     met_guess  oz
prse     61     0     met_guess  prse
ps        1     0     met_guess  prse
sst       1     0     met_guess  sst
cw        60     1     met_guess  cw
ql        60     1     met_guess  ql
qi        60     1     met_guess  qi
qr        60     1     met_guess  qr
qs        60     1     met_guess  qs
qg        60     1     met_guess  qg
qh        60     1     met_guess  qh
::

```

6.3 Presentations

Wu, T.-C. 2018: A DTC Visitor Program Project: Evaluating and Merging the Capability of Assimilating Satellite Hydrometeor Retrievals into GSI for HWRP Application. EMC GSI Bi-Weekly Meeting, February 21st, 2018, College Park, MD.

Wu, T.-C., M. Zupanski, L. Grasso, C. Kummerow, and S.-A. Boukabara, 2017: Assimilation of Microwave Hydrometeor Retrievals and All-Sky Radiances in HWRP. 18th Annual WRF User's Workshop, June 15th, 2017, Boulder, CO.

7. Reference

- Aligo, E., B. S. Ferrier, J. Carley, E. Rogers, M. Pyle, S. J. Weiss, and I. L. Jirak, 2014: Modified microphysics for use in high resolution NAM forecast. *27th AMS Conference on Severe Local Storms. 3-7 November, Madison, WI.*
<https://ams.confex.com/ams/27SLS/webprogram/Paper255732.html>.
- Biswas, M. K., and Coauthors, 2017: Hurricane Weather Research and Forecasting (HWRP) Model: 2017 Scientific Documentation. *Dev. Testbed Cent.*, 1–97.
http://www.dtcenter.org/HurrWRF/users/docs/scientific_documents/HWRPScientificDocumentation_August2011.pdf.
- Brown, P. J., C. D. Kummerow, and D. L. Randel, 2016: Hurricane GPROF: An optimized ocean microwave rainfall retrieval for Tropical Cyclones. *J. Atmos. Ocean. Technol.*, **33**, 1539–1556, doi:10.1175/JTECH-D-15-0234.1.
- Kummerow, C. D., D. L. Randel, M. Kulie, N. Y. Wang, R. Ferraro, S. Joseph Munchak, and V. Petkovic, 2015: The evolution of the goddard profiling algorithm to a fully parametric scheme. *J. Atmos. Ocean. Technol.*, **32**, 2265–2280, doi:10.1175/JTECH-D-15-0039.1.
- Wu, T.-C., and M. Zupanski, 2017: Assimilating GPM hydrometeor retrievals in HWRP: choice of observation operators. *Atmos. Sci. Lett.*, **18**, 238–245, doi:10.1002/asl.748.
- , ———, L. D. Grasso, P. J. Brown, C. D. Kummerow, and J. A. Knaff, 2016: The

GSI Capability to Assimilate TRMM and GPM Hydrometeor Retrievals in HWRP.
Q. J. R. Meteorol. Soc., **142**, 2768–2787, doi:10.1002/qj.2867.

——, ——, ——, C. D. Kummerow, and S. A. Boukabara, 2018: All-Sky Radiance
Assimilation of ATMS in HWRP: A Demonstration Study. *Mon. Weather Rev.*,
(Accepted with Revisions).